STOCHASTIC VERSUS CHAOTIC DYNAMICS FOR GENETIC MODEL — REVISITED*

A. KLECZKOWSKI**

Department of Zoology, University of Cambridge
Downing Street, Cambridge CB2 3EJ, England

(Received June 6, 1993)

The stroboscopic maps technique is applied to a model of the dynamics of a single haploid population with a natural selection in a fluctuating environment (genetic model). The stochastic perturbation is replaced by a deterministic chaotic system which — in a certain limit — has properties of a white noise generator. First, the white noise limit is discussed and tested using various statistical methods. The transition from the deterministic chaotic behaviour to the stochastic one, depending on the time scales separation is discussed. We also discuss the results of using different underlying chaotic dynamics on the macroscale properties, especially Lyapunov exponents and dimensions. The paper forms a revision and a substantial extension of [1].

PACS numbers: 05.45. +b

1. Introduction

Systems exhibiting chaos properties can be analyzed by both deterministic and stochastic methods [2]. It is also possible to find systems explicitly showing this "dualism", *i.e.* in some limit exhibiting purely deterministic, chaotic motion, but in another limit modelling a stochastic process (having *e.g.* correct moments and correlation functions [3, 4]). Such models are especially interested, because they can offer a deeper insight into a mechanism of generating stochastic processes in nature. Throughout the paper we will call the limit process as a "stochastic" one, realizing that in principle it is generated by the underlying deterministic process. This can be done,

* This work was partially supported by the Polish KBN Grant 2.0387.91.01.

** On the leave of absence from Institute of Physics, Jagellonian University, Reymonta 4, 30-059 Kraków, Poland.

if we show which actual properties of a "really stochastic" process can be mimicked by the process, and to what extend.

In the paper we follow the ideas of [3], and use a simple chaotic map as an input for another discrete dynamical system which — finally — produces a time series of uncorrelated random numbers with Gaussian distribution. This approach provides us with a random numbers generator, for which all characteristics may be calculated analytically [2–4].

Then, we consider a case when the process underlying the random number generation is not treated as an artificial construction, but as a real process, which however cannot be observed directly, but only through its influence onto a "macroscopic" level dynamics. Depending on the time scales separation, the transition from the deterministic to the stochastic behaviour can be observed, and therefore discussed.

In the paper we are studying the influence of such "pseudo-stochastic" (chaotic) perturbations on the population dynamics of a single haploid population, with a natural selection provided by a fluctuating environment. The simple model known in literature as "genetic model" has been extensively investigated from different points of view, and its applications are not limited to the population dynamics. In fact, the model is the simplest nonlinear system, which can be treated therefore as a "model system" for more complicated physical, chemical, and biological systems. The deterministic and stochastic properties are well known from the analysis carried out by Horsthemke and Lefever [5] in the frame of the stochastic processes theory. The results of this paper form a substantial extension and revision of the chapter 3 of [1].

Systems with complicated time- and coordinate-dependence can be easily analyzed by the stroboscopic maps method joined with the singular ("kicks") approximation [6]. In this approach, the time-dependent perturbation, originally not having the impulse form, is approximated by a series of "kicks" (δ-functions) with the distance between the impulses tending to 0 [7, 8]. This technique may be applied either to regular or to stochastic perturbations. The first case, when a regular, time-dependent perturbation is replaced by series of kicks, is known in quantum optics as the Modulated Kicks Approximation (shortly MKA) [7–11]. For a stochastic perturbation, this approach was first formulated by Langevin and Haken [12–15]. Special kind of such a perturbation with a finite distance between kicks is known as a "shot noise" [13, 16] and has been studied extensively by many authors [17–19]. In particular, van den Broeck has shown that — under some assumptions — a certain kind of a shot noise tends to a Gaussian white noise when the (mean) distance between kicks tends to zero [16]. The method simplifies the analysis by making at least part of the work analytically solvable, even if the original system cannot be analyzed by other methods (including

Fokker–Planck equation). The resulting map is naturally adjusted to the discrete-like perturbation, which is typical for studying the chaotic systems (Poincaré maps, discrete maps [20]).

In the paper, we construct the stroboscopic map for the genetic model, basing on the results of [6]. The results published in [1] were obtained under the assumption that the impulses are sufficiently short, and that we can neglect the changes of the perturbation during the impulse. The subsequent detailed analysis of the systems with impulses in [6] has shown that the above assumption is wrong for systems like the genetic model (although gives good approximation of the results for small perturbation). Moreover, the chaotic (sub)system used in [1] produced the Ornstein–Uhlenbeck process in the limit, and not the white noise, and the comparison with the exact (stochastic) results are difficult in this case. The (sub)system used here has additional degrees of freedom, allowing us to discuss the transition in more details.

First, we shortly review the basic methods used here, *i.e.* the genetic model, the Generalized Modulated Kicks Approximation, the stroboscopic maps approach, and the chaotic (sub)system generating the noise (Section 2). Then we proceed to discuss the results of the simulations for the white noise limit, and for the transition (Section 3). Section 4 contains some remarks on using different chaotic systems, whereas Section 5 reviews the chaotic characteristics. Section 6 gives final remarks.

2. Basic elements

2.1. Genetic model

The genetic model (Fisher–Wright's model) describes the mechanism of genetic selection in population dynamics for a single haploid population. We will concentrate on the continuous version (a limit case of a Markov chain approach). The system is very simple, and was analyzed thoroughly from both deterministic, and stochastic point of view. However, when perturbed by noise, it exhibits a transition in modality of its probability distribution when the noise amplitude exceeds a certain limit ("noise-induced transition").

After several simplifications and assumptions [1, 5, 21] it can be shown that the frequency (x) of a given allele changes from generation to generation according to the equation

$$\dot{x} = \alpha - x + \lambda x(1-x), \tag{1}$$

where α is related to mutation rates of two possible alleles of a genetic locus and λ to natural selection coefficients.

The system can also be understood as describing a concentration of a chemical substrate $\mathcal{X}$, put into a flow reactor with the speed α, and undergoing the following reactions

$$\xrightarrow{\alpha} \mathcal{X} \xrightarrow{\alpha} \mathcal{Y} \xrightarrow{\alpha}$$
$$\mathcal{X} + \mathcal{Y} \xrightarrow{\lambda} 2\mathcal{X},$$

where $\mathcal{Y}$ is taken out from the reactor with the same speed α, so $x + y = 1$ with y being a concentration of $\mathcal{Y}$, and the second reaction is characterized by λ.

Without a loss of generality α may be fixed as $1/2$ [5]. It is easy to check that x lies always inside the interval $[0, 1]$. When $\lambda = \text{const}$, Eq. (1) has only one stable state, namely $x_{ss} = [\lambda - 1 + (\lambda^2 + 1)^{1/2}]/(2\lambda) = 1/2$.

If an environment becomes fluctuating and the selection coefficients become stochastic variables, the deterministic steady state may lose its stability. When a critical value of the fluctuations of λ is exceeded, two new states appear, close to 0 and 1. For the white noise perturbation with zero mean and variance σ^2_{WN}, the transition from the unimodal probability distribution of x to the bimodal one occurs at $\sigma^2_{cr} = 4$ (Stratonovich interpretation), and new maxima have positions $x_{m\pm} = 1/2\,[1 \pm (1 - 4/\sigma^2_{WN})^{1/2}]$ [5].

2.2. Stroboscopic maps for system with impulses

Eq. (1) belongs to a class of 1-dimensional dynamical systems

$$\dot{x} = f(x) + \lambda(t)g(x), \tag{2}$$

where $f(x)$ determines a free (unperturbed) evolution and $\lambda(t)g(x)$ is a time- and coordinate-dependent perturbation (regular, chaotic, stochastic, continuous or impulse). There are several methods for solving this equation, depending on the character of $\lambda(t)$. For $\lambda(t)$ being a noise, it is possible to employ the methods of the stochastic theory (*e.g.* Fokker–Planck equation) to analyze the time-dependent and stationary properties of (2); for a review *cf.* [1, 5, 17–19].

Let us concentrate on the case with general $\lambda(t)$ (deterministic or stochastic). One of the methods of analysis [6] approximates $\lambda(t)$ by a series of infitely short impulses with the weight and centers chosen according to the type of $\lambda(t)$ (see below). Then, it is possible to integrate Eq. (2) both between the impulses (assuming that the equation $\dot{x} = f(x)$ can be solved easily), and during the impulse (assuming that the equation $\dot{x} = g(x)$ can be solved), basing on the fact that the impulses are very short [6]. The resulting map depends on the (arbitrary to some extend) division between $f(x)$ and $g(x)$. Both [1] and [6] assume $f(x) = 1/2 - x$, and $g(x) = \lambda(t)x(1 - x)$.

More natural choice, dictated by the stochastic theory, is to divide the right hand side into a drift term $f(x) = {}^1\!/_2 - x + \lambda_0 x(1-x)$, and a diffusion term $g(x) = (\lambda(t) - \lambda_0)\, x(1-x)$. As we will assume that the mean value of the noise (time-dependent) perturbation is 0, both cases produce the same result, namely

$$\begin{cases} x_n^- = \frac{1}{2}(1 - \exp(-T)) + x_{n-1}^+ \exp(-T) \\ x_n^+ = \dfrac{x_n^-}{x_n^- (1-\exp(-\lambda_n)) + \exp(-\lambda_n)}, \end{cases} \tag{3}$$

if the perturbation $\lambda(t)$ has the following form

$$\lambda(t) \sim \Lambda(t) = \zeta(T) \sum_n \lambda_n \delta(t - t_n), \tag{4}$$

where t_n are moments in time, ordered ($t_n > t_{n-1}$ for all n), $t_n - t_{n-1} = T_n$ may be a constant ($T_n \equiv T$), a regular or a stochastic function of n, impulses are assumed to be well separated, *i.e.* $T_n > \Delta$ for all n, and $\zeta(T)$ is a scaling function discussed below in details. The above map will be called the gentic map throughout the paper.

The following notation has been used here

$$\begin{cases} x_n^+ = x(t_n + \frac{\Delta}{2}) \\ x_n^- = x(t_n - \frac{\Delta}{2}), \end{cases} \tag{5}$$

reflecting the fact that as the impulses form the reference system of moments in time, they make it natural to consider values of the dynamical variable x at times correlated with the impulses. This leads us to a concept of a stroboscopic map, being in fact a discrete transformation

$$\ldots \to x_{n-1}^+ \to x_n^- \to x_n^+ \to \ldots .$$

The stroboscopic map is especially suited if the perturbation can be thought of as a discrete transformation (map), or if we assume that the environment acts upon the system at certain times only. This may actually be true for the case of a genetic selection, when there are critical moments in the life–history of one generation.

The result (3) differs from Eq. (1.11) of [1], because the "naive" way of integrating the equation (1) during the impulse, assuming that $g(x)$ does not change, was used there. In fact, x, and therefore $g(x)$ has a jump at every t_n, and the equation becomes singular. The only correct way to treat this problem is to use continuous approximations of $\delta(t)$ functions, *cf.* [6].

2.3. *Singular approximation*

In the above considerations we have approximated $\lambda(t)$ by a series of impulses. Now, the correct weights λ_n and points in time t_n need to be chosen in order to model $\lambda(t)$ correctly.

For regular $\lambda(t)$ the most natural choice is $t_n - t_{n-1} = \text{const} = T$ and $\lambda_n = \zeta(T)c(t_n)$, with $\zeta(T)$ being a scaling function needed to keep chosen characteristics of $\lambda(t)$ and the approximation the same, independently of T. The compatibility criterion is usually defined in terms of an integral of $|\lambda(t)|$ and a sum of $|\lambda_n|$. This leads to the scaling $\zeta(T) \sim T$. For stochastic perturbations there are two basic ways: one can chose $t_n - t_{n-1} = T_n$ to be a stochastic variable with λ_n oscillating between two values (shot noise). In this case the limiting procedure is defined for the mean value and variance of T_n (going both to 0). The other approach is based on the assumption that the impulses are equidistant ($T_n = \text{const} = T$ with $T \to 0$), but the amplitude is a random variable. In both cases the scaling is usually based on the autocorrelation functions for $\lambda(t)$ and λ_n. This leads to the scaling law $\zeta(T) \sim T^{1/2}$. The second approach was chosen by Beck and Roepstorff [3] and, as we follow them in construction of the random number generator in the application, we choose this one.

2.4. *Chaotic random number generator*

In our paper we focus on the white noise simulations. Following [3, 4] we consider a function $S_\tau(t)$ built from the step (piecewise constant) functions

$$\begin{cases} S_\tau(t) = \tau^{1/2} \sum_{k=0}^{\lfloor t/\tau \rfloor} \mathcal{F}(v_k) \\ v_k = (\mathcal{T}^k v_0)\,, \end{cases} \tag{6}$$

where $\mathcal{T}$ is a discrete dynamical system with certain properties (ϕ-mixing, *cf.* [3]), v_0 a number (or a vector of numbers; in the latter case, when $\mathcal{T}$ is multidimensional, we take one component into the first equation of (6), τ a characteristic time and $\lfloor t/\tau \rfloor$ denotes the integer part of t/τ. Then in the limit $\tau \to 0$, S_τ converges to a Wiener process with σ^2_{WP} depending on $\mathcal{F}$ and $\mathcal{T}$ (where $E(S_\tau(t)^2) \to \sigma^2_{WP} t, \tau \to 0$ and $E(.)$ denotes a mean value). For a simple choice (analyzed in details by Beck [3]) $\mathcal{F}(v) = v$ and $\mathcal{T} v_{k-1} = 1 - 2\,v^2_{k-1}$ we get $\sigma^2_{WP} = {}^1\!/_2$.

Then, the Gaussian white noise with the same $\sigma^2_{WN} = \sigma^2_{WP}$ may be generated as a "derivative" of the Wiener process with respect to time. The derivative must be, however, applied to a limit process $\tau \to 0$, but can be approximated by a difference of the values at times separated by $T \gg \tau$

$$L_{\tau,T}(t) = \tau^{1/2} \sum_{k=0}^{\lfloor t/\tau \rfloor} (v_k - v_{k-p})\, \delta(t - \tau_k)\,, \tag{7}$$

where $\theta_n = n\tau$, and $p = \lfloor T/\tau \rfloor$; $\tau \to 0$ and $T \to 0$ with $p^{-1} \to 0$.

There are three different time scales in the system, the "fastest" scale τ of the underlying chaotic process, the "slow" scale T of the "derivative", and the natural time scale of the process which is perturbed by the noise. The proper white-noise limit requires a clear separation of the time scales. Such a separation cannot be achieved in reality, and therefore it seems interesting to investigate the properties of the system when the limits are approximate only.

Eq. (7) can be rewritten in the "propagator" form [1]

$$L(t) \sim T^{1/2} \sum_n l_n\, \delta(t - t_n)\,, \tag{8}$$

where $t_n = nT$ and

$$l_n \equiv p^{-1/2} \sum_{k=1}^{p} v_{n-k}\,. \tag{9}$$

Here we substitute $\tau = T/p$ and relate the scaling by T with the impulse character of (8).

Statistical properties of l_n can be found under the assumption of the ϕ-mixing of $\mathcal{T}$, and by applying weaker versions of the Central Limit Theorem [2, 3, 22]. "Oversampling" ($p > 1$) guarantees that the probability distribution of l_n tends to a Gaussian one with mean 0 and variation σ^2_{WN} (equal $1/2$ in the simplest case presented here) when $p \to \infty$ (this property was first discussed by Lewenstein and Tél [23]). For small p, the one-point distribution is close to the invariant measure of the chaotic process $v_k = \mathcal{T} v_{k-1}$, as in the case $p = 1$ ($1/\sqrt{\pi\, x(1-x)}$ for the logistic map [20]), although the variance may remain the same as it happens in the simplest case presented here. Indeed, if we use the formula

$$E(l_n^2) \overset{p\to\infty}{\longleftarrow} E(v_n^2) + 2 \sum_{k=1}^{p} E(v_n v_{n-k})\,, \tag{10}$$

(*cf.* [3]) we see that for the uncorrelated maps $\mathcal{T}$, *i.e.* for which $E(v_m v_n) = \delta_{m,n}$, $E(l_n^2) = E(v_n^2)$ coincides with the variance for $p = 1$.

The p-dependence of the mean value and variance of l_n was checked, for a large range of p. As expected, both characteristics do not depend on p, *cf.* [1, 2]. On the other hand, the probability distribution (histogram) of

l_n depends highly on p, but for $p = 100$ the distribution approximates well the Gaussian one. In [1] the estimations of the third and fourth moments (skewness and kurtosis) are given for the similar model (Ornstein–Uhlenbeck process). Both characteristics reach the Gaussian values in the limit equivalent to our $p \to \infty$. However, higher moments tend to have large errors, and are usually not recommended as normality tests [24].

The time series resulting from the iterations of Eq. (9) (n ranging from 1 to 2000, and p ranging from 1 to 200, meaning the total number of iterations of $\mathcal{T}$ from 2000 to 400000) was tested for normality of the one point distribution, as well as for the lack of correlations (whiteness). For both statistical test we have chosen the Kolmogorov–Smirnov test. The comparison with the normal distribution is a standard one–sample test, for which Kolmogorov–Smirnov test is recommended [25]. On the other hand, there are several white-noise tests. Bartlett [26, 27] suggested the comparison of the standardized partial sums of the periodogram with the cumulative distribution function of a uniform distribution, again by the Kolmogorov–Smirnov test. This test looks for maximum difference in the spectrum of a given time series from the constant spectrum (white noise).

Fig. 1, and Fig. 2 show the results of the statistical analysis of the shape of the one point distribution for different values of $p = 1$, and 100, respectively. The figures contain, respectively: *Time series* — the first 200 iterations of Eq. (9); *Histogram* — the one-point distribution (divided into 32 bins); *Quantiles* — a quantile–quantile plot of the distribution *vs.* the normal distribution (the line represents the best fit); *Distribution functions* — a plot of two Empirical Distribution Functions as being compared in the Kolmogorov–Smirnov test, solid line representing the distribution of time series, dashed — the normal distribution. On both of the last two plots, the lines representing the measured and the normal distributions should coincide. The Kolmogorov–Smirnov test takes the maximum difference between both lines to calculate the statistics.

Fig. 3 and Fig. 4 present test results for the white noise. The figures show, respectively: *Delay plot* — presents the first return map (x_{n+1} *vs.* x_n); *Autocorrelation* — the autocorrelation function of the time series, with the zeroth mode removed (it is always equal 1) and with an approximate 95% confidence intervals; *Power spectrum* — the results of spectral analysis; and *Distribution function* — standardized partial sums of the periodogram (solid line) and the cumulative distribution function of a uniform random variable (dashed line), as required in the Bartlett's Kolmogorov–Smirnov test.

Fig. 5 summarizes the results. It contains the probability values calculated from the Kolmogorov–Smirnov statistics for the normality test (filled squares) and white–noise test (crosses), as functions of p. The horizontal

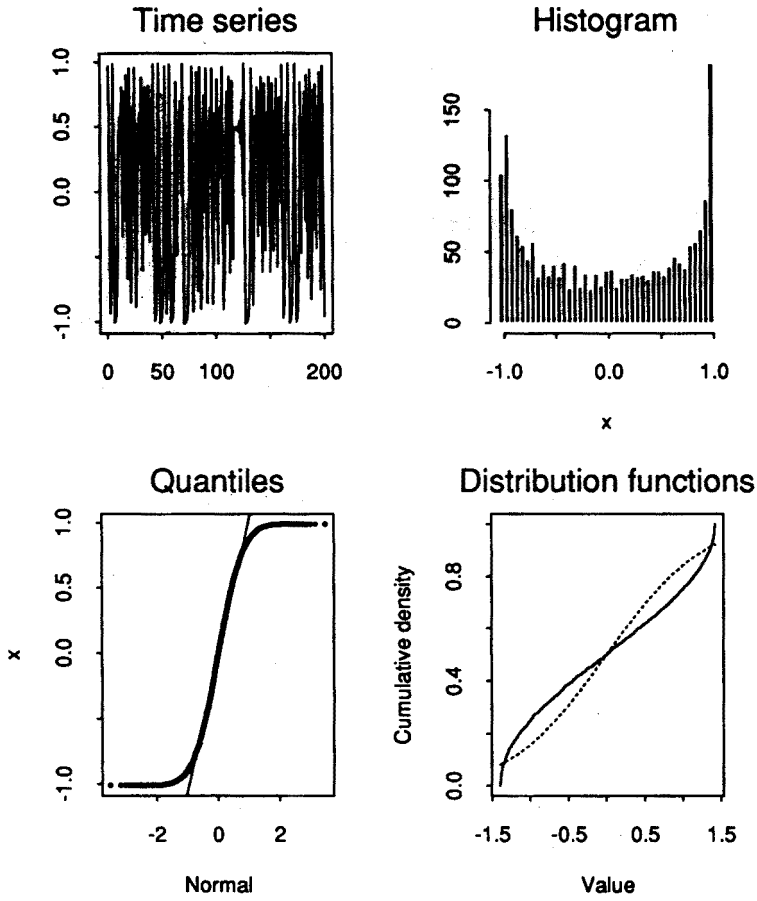

Fig. 1. Statistical analysis of the one point distribution for the chaotic (sub)system with $p = 1$. For the description, see text.

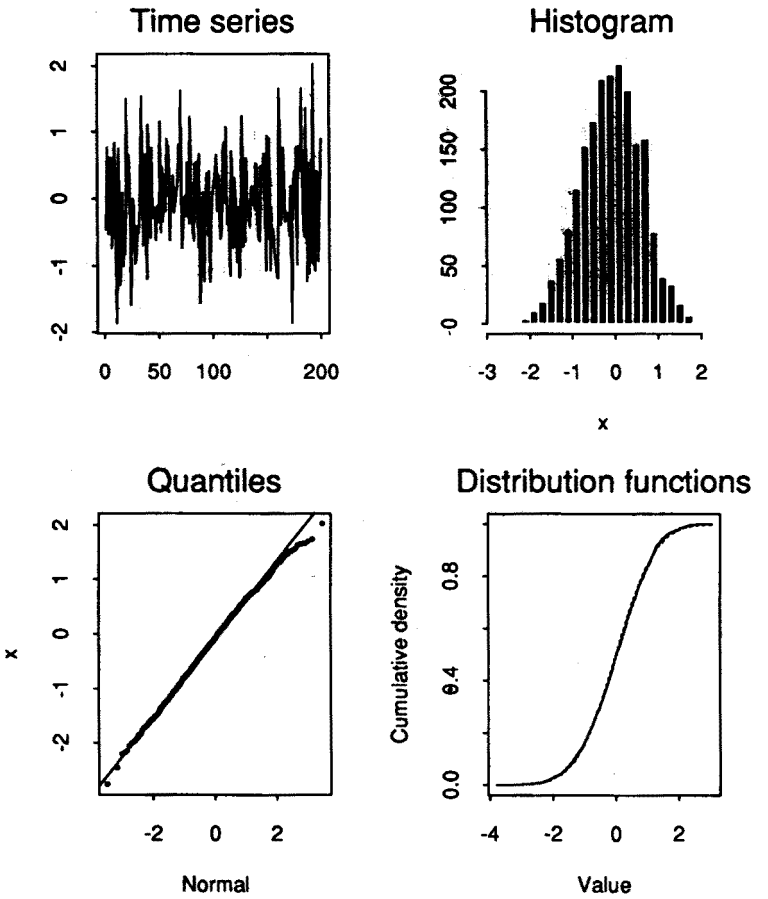

Fig. 2. The same, as before, but for $p = 100$.

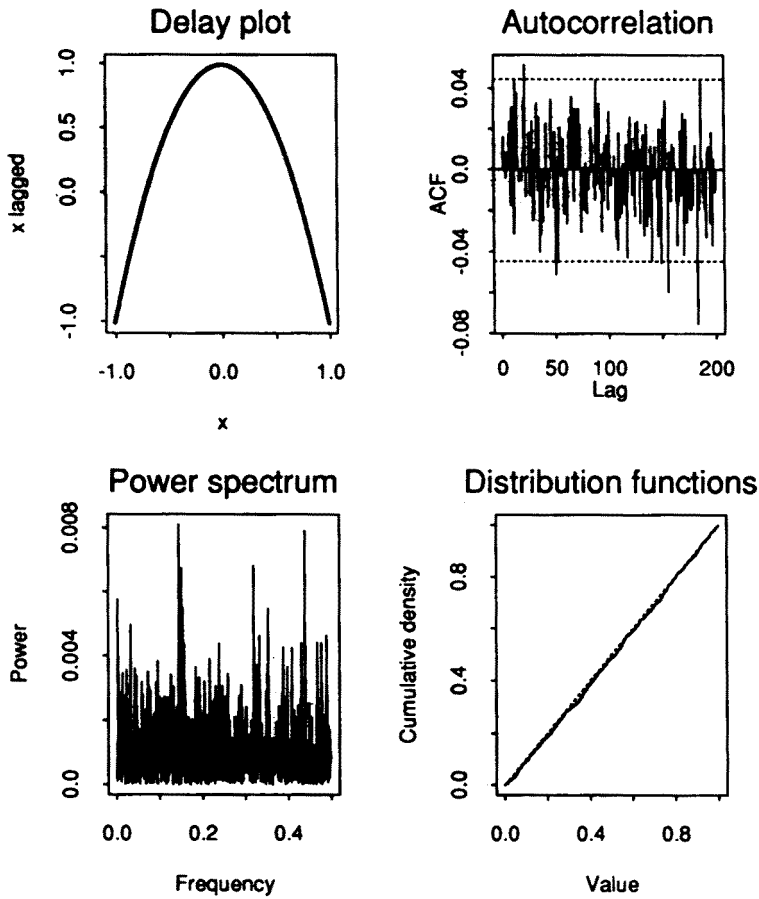

Fig. 3. Statistical analysis of the time series generated by the the chaotic (subsystem) with $p = 1$. For the description, see text.

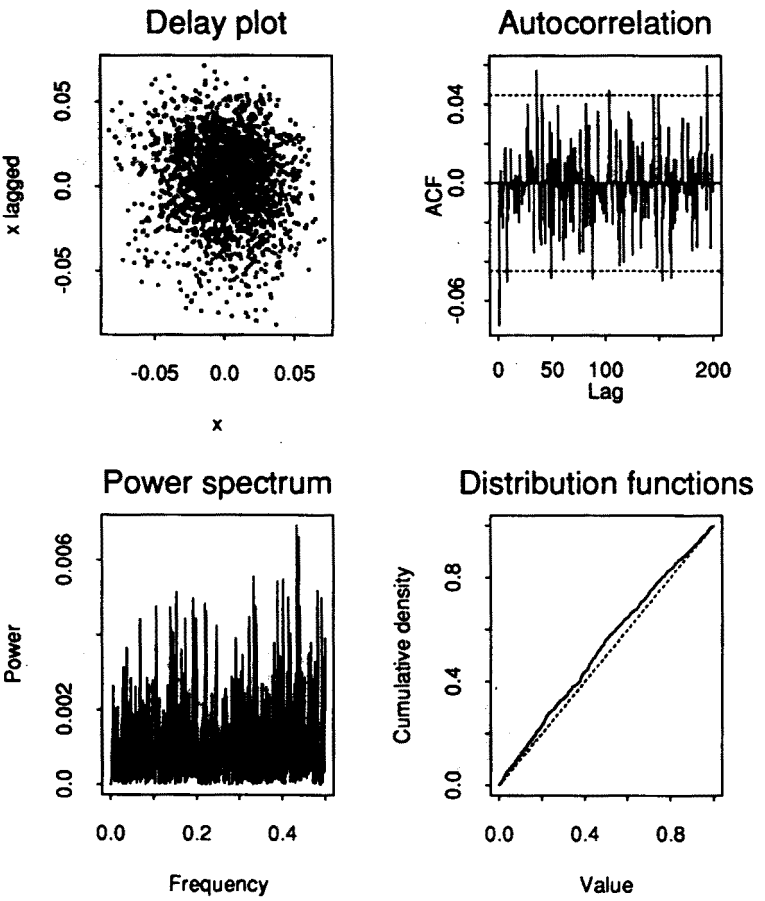

Fig. 4. The same, as before, but for $p = 100$.

lines represent $Prob = 0.01$ and 0. As the tests involve relatively large samples (2000), they are very sensitive and tend to overemphasize small differences in the (empirical) distribution functions. Nevertheless, it is clear that the Gaussian limit is reached for large p, and the spectrum is not significantly different from the uniform one for (almost) any p. The autocorrelation functions do not contain values significantly excceding the 95% confidence intervals.

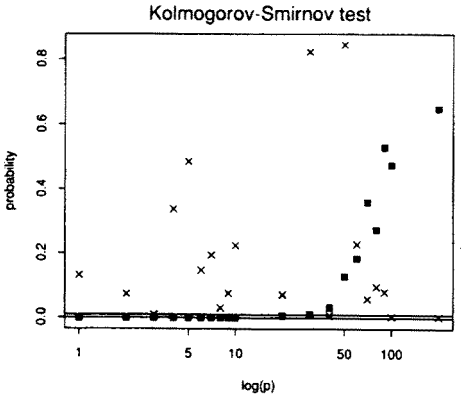

Fig. 5. Kolmogorov–Smirnov probabilities for significance tests: Gaussian (■), white-noise (×), described in the text.

Finally, it should be noted that the delay pictures in Fig. 3 and Fig. 4 can be compared with the respective figures in the next chapter for the genetic model.

2.5. Genetic map — simulations

The map (3) was iterated with $\lambda_n = \epsilon\, l_n$ and with $\zeta(T) = T^{1/2}$ (cp. (8)). With the time n running, the histogram of x_n^+ (called x below) saturates to represent the natural measure of the discrete dynamical process given by (3).

First we compare the results of the simulations for different p and T with ϵ fixed. Changes in p affect only the shape of the probability distribution of the perturbation (λ_n) and the amplitude of noise does not depend on p. As a result, the mean value and the deviation of x are also p–independent, but the shape of the probability distribution depends substantially on p, especially for small p.

The situation is completely different for T. Although again the mean value of x is independent of T (up to some fluctuations), the deviation decreases with decreasing T linearly tending to a certain value σ_0. When σ_x is plotted as a function of $\ln(T)$, see Fig. 6, the curve saturates below

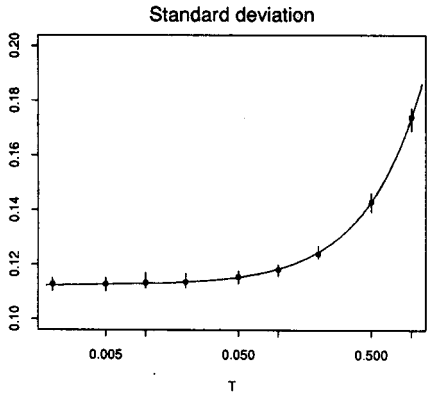

Fig. 6. Standard deviation for the distribution of x^+ *vs.* T. Bars represent the minimal and maximal value of σ^2 among 50 runs starting from different initial conditions. The line represents the least–square fit.

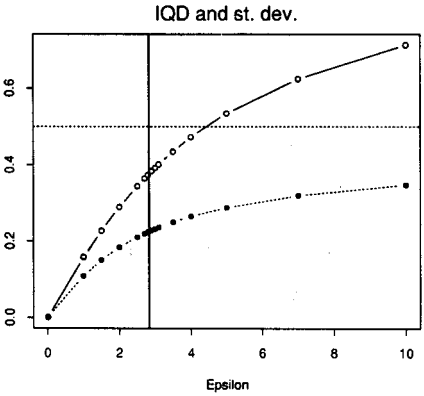

Fig. 7. Standard deviation and the interquartile distance (interval containing 50% of the probability, which is more robust characteristic of spread of a distribution, if the latter is not Gaussian) of the probability distribution of x^+ *vs.* noise strength. The horizontal line shows the maximal value of the standard deviation 0.5, and the vertical line represents the thoretical transition point 2.828..., corresponding to $\sigma^2 = 4$ (o — IQD, • — st. dev.).

$T \simeq 0.05$ (for $\epsilon = 1.0$). This suggests that the values of T of order of 0.01 and less are sufficient to model the behaviour of the genetic model (smaller T requires longer runs).

Fig. 7 shows the dependence of the deviation σ_x on ϵ as well as some examples of histograms of x. It is not easy to determine the exact point at which the transition occurs, as σ_x changes smoothly for all ϵ (no "sharp" transition), and the histograms are subject to fluctuations. Nevertheless, the lower and upper bounds may be estimated, with $\epsilon = 2\sqrt{2} \simeq 2.828...$

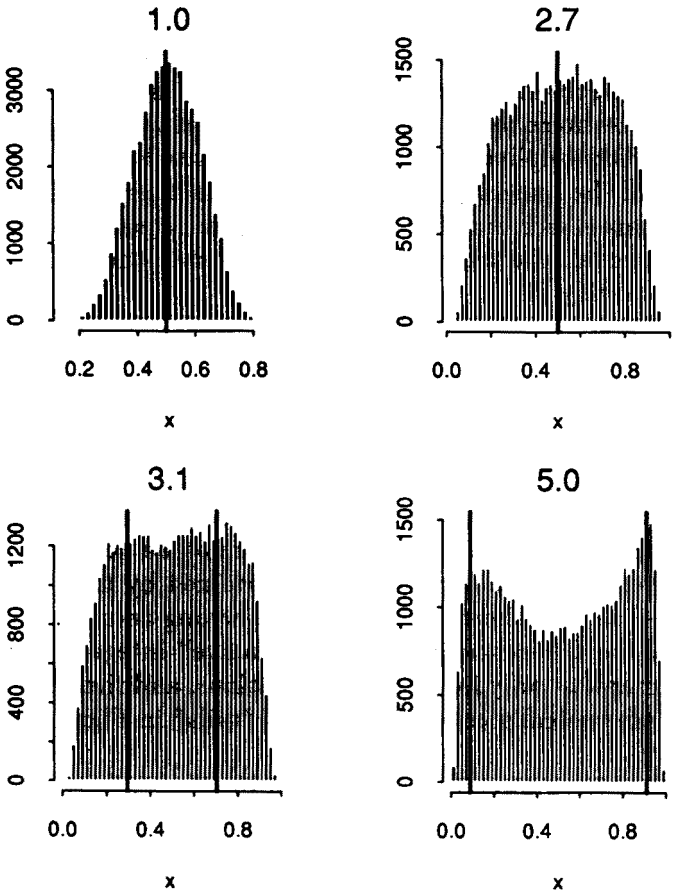

Fig. 8. Histograms of the distribution for different ϵ ($T = 0.01$, and $p = 100$). Vertical lines mark the theoretical location of the maxima.

inside the interval (corresponding to $\sigma^2 = 4$) . The mean value fluctuates around $^1/_2$. $p = 100$, $T = 0.01$, and the genetic map was iterated 50000 times.

The figures Fig. 8 shows the examples of the histograms (32 bins) for small $\epsilon = 1$, short before the transition (2.7), short after the transition (3.1), and for large amplitude (5.0).

If Eq. (1.11) of [1] is used instead of Eq. (3), the probability distribution is no longer bound by 0 and 1, *cf.* the figure 4 in [1], suggesting that the interpretation of x as a population density is no longer possible. Plotting and comparing both maps, one can easily see that the effect is caused by the rare events in the noise realization when the actual value of the perturbation λ_n is large. With amplitude ϵ growing, this events become more and more important, and the trajectories "flow" out of the interval. This is no longer true for our map — as it is not true for the original equation — and if started in the unit interval, the trajectory will always stay there. This problem is discussed separately [6].

3. Transition from chaos to a stochastic limit

The genetic model has been used in [1] in order to investigate the transition properties of the systems from the chaotic to stochastic regime of dynamics. However, the results obtained there apply to the Ornstein–Uhlenbeck process, where the transition cannot be controlled very easily (one parameter γ). Moreover, they were obtained by the "naive" integration, which — as it is shown in [6] — gives wrong results. As it has been proved there, the differences between the "naive" integration and the correct method manifest only for large perturbations, and therefore the pictures shown in [1] are basically correct (except of "tails" in Figs 10–12, above 1.0 and below 0.0).

Similar problems have been addressed in [3, 4]. In this approach the deterministic systems generating the stochastic process approximation are treated literally (not only as a limit case). The idea introduced by Beck and Roepstorff [3] and developed in [1, 2, 4, 22, 28] that some of the stochastic processes might have their origin in a purely deterministic, but chaotic behaviour can also be applied here.

The transition from the deterministic motion to the stochastic (Gaussian white noise) limit is realized by the change of p and T ($p \to \infty$ and $T \to 0$). We can treat the maps (3) with (9) as chaotic maps, and analyze the structures of the attractor in a delayed phase space. Below we will concentrate on the analysis of the attractor in a 2-dimensional space, equivalent to the map x_n^+ *vs.* x_{n-1}^+.

In order to understand better the transition, let us focus on p-dependence

first, and go with $T \to \infty$. In this limit Eq. (3) is reduced to one equation for x_n^+

$$x_n^+ \sim \frac{1}{1+\exp(-\lambda_n)}. \tag{11}$$

For small perturbations λ_n, x_n^+ is a linear function of λ_n, *i.e.* $x_n^+ \sim 0.5 + 0.25\lambda_n$. If, in addition, $p = 1$, the map x_n^+ *vs.* x_{n-1}^+ can be written in a closed form without λ_n, depending on $\mathcal{T}$, *cf.* (6). For the logistic form of $\mathcal{T}$, the map is a parabola, as shown in Fig. 3. For p increasing, the map becomes more and more complicated (higher iteratives of $\mathcal{T}$, as well as "memory" effects become involved). As it was shown in [3], in the limit $p \to \infty$, λ_n becomes a Wiener process, and the map x_{n+1}^+ *vs.* x_n^+ loses any internal structure.

On the other hand, if $T \to 0$, $x_n^- \sim x_{n-1}^+$, and

$$x_n^+ \sim \frac{x_{n-1}^+}{x_{n-1}^+(1-\exp(-\lambda_n)) + \exp(-\lambda_n)}. \tag{12}$$

Again, for small λ_n, the map for x^+ can be easily found

$$x_n^+ \sim (1+\lambda_n)\, x_{n-1}^+ - \lambda_n\, (x_{n-1}^+)^2\,. \tag{13}$$

For λ_n visiting the points from the certain interval (for $p \to \infty$ it is $-\infty \ldots +\infty$), the points of the map are lying on the momentary curves given by (13). If the λ_n points are dense in the certain interval (λ_-, λ_+), the map of x^+ fills an area between appropriate curves. The section of the probability distribution on this area along a line $1 - x_n^+$ is a rescaled probability distribution of λ_n (*i.e.* $\sqrt{2}/\,8\,\lambda_n + \mathcal{O}(\lambda_n^2)$). This can be compared with the λ_n-distributions obtained by Beck [3, 4, 28], see also above.

Fig. 9 presents a series of plots for different p and large T, whereas Fig. 10 shows similar figures for small T.

As mentioned above, p controls the probability distribution of the noisy perturbation. The attractor does not change significantly if p is changed for small T, although there are changes in the structure of the cross-section, and on the boundaries, which become more spread. On the other hand, large values of T lead to a completely deterministic picture with more and more structure added as p becomes larger. At some value of p, depending on T and ϵ, the picture becomes indistinguishable from noise.

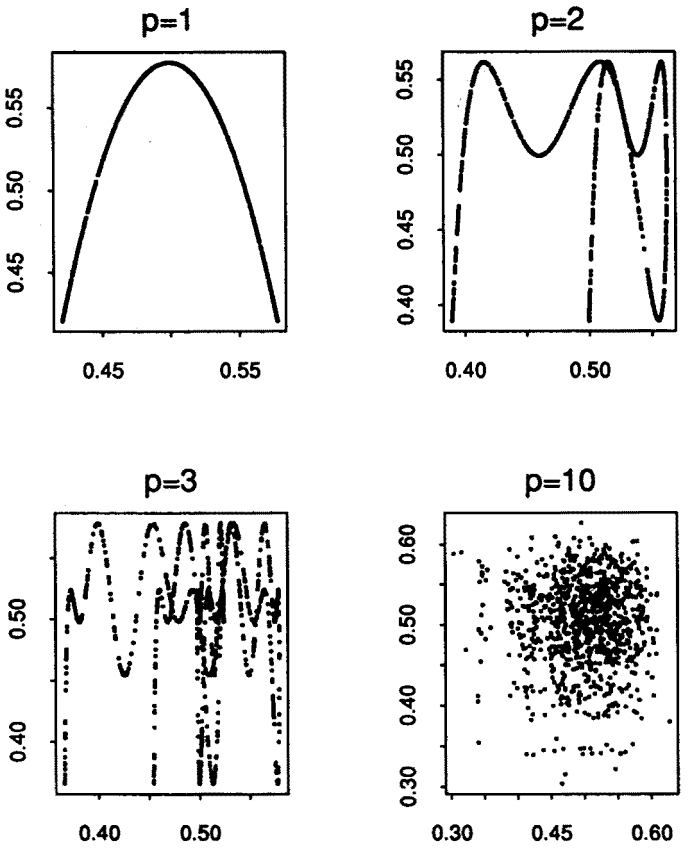

Fig. 9. Plots of the attractor for the genetic map for $p = 1$, $p = 2$, $p = 3$, and $p = 10$ with $T = 100$. $\epsilon = 0.01$ and 1000 points are plotted for each attractor.

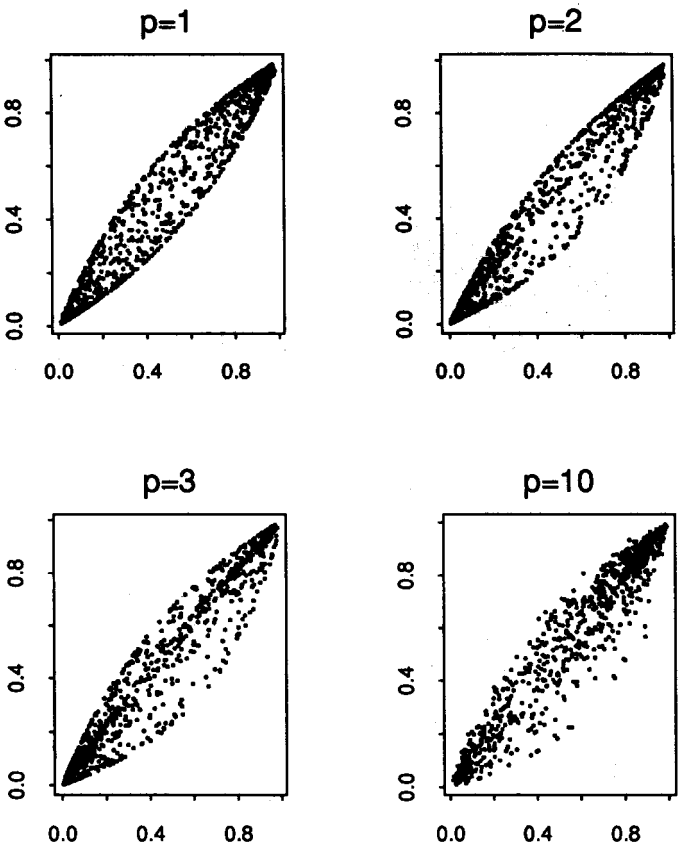

Fig. 10. The same as above, but for $T = 0.01$, and $\epsilon = 7$.

4. Other chaotic systems

The probability distribution of the logistic map for $a = 2.0$ is smooth and simple. The system at this point possesses some properties which makes it possible to prove the limit theorem [3], *e.g.* complete lack of correlation

between subsequent iterates. The conclusions of the theorem remain, however, true even if the assumptions are relaxed. As long as the correlations in the chaotic time series are shorter than p, a good approximation of the white noise can be generated by Eq. (7).

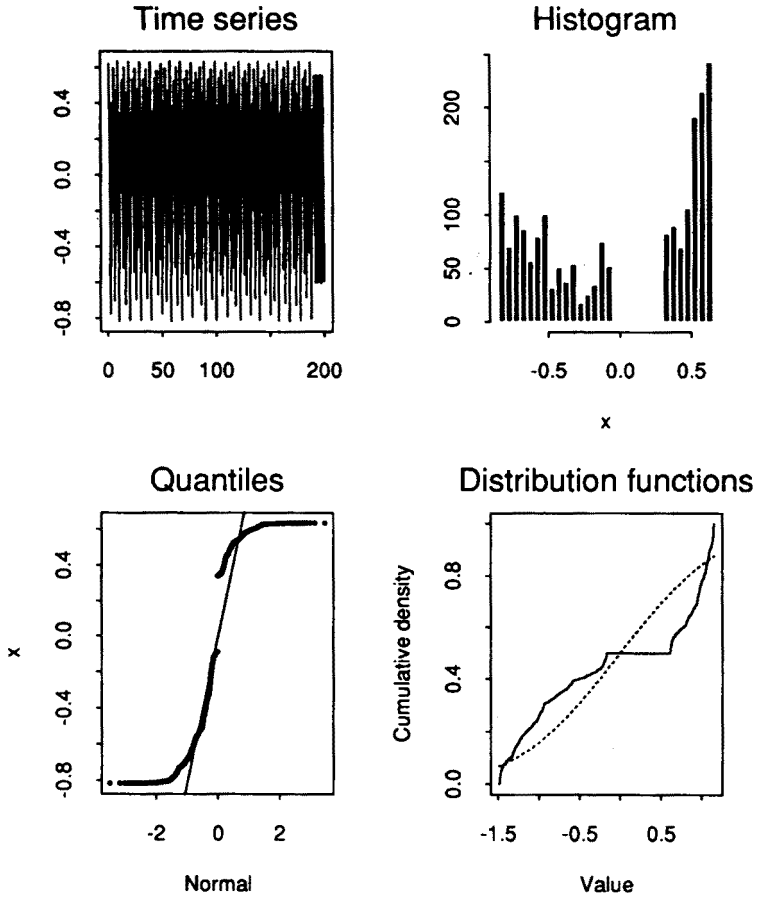

Fig. 11. Statistical analysis of the probability distribution, $a = 1.45$ and $p = 1$. For the description, see text.

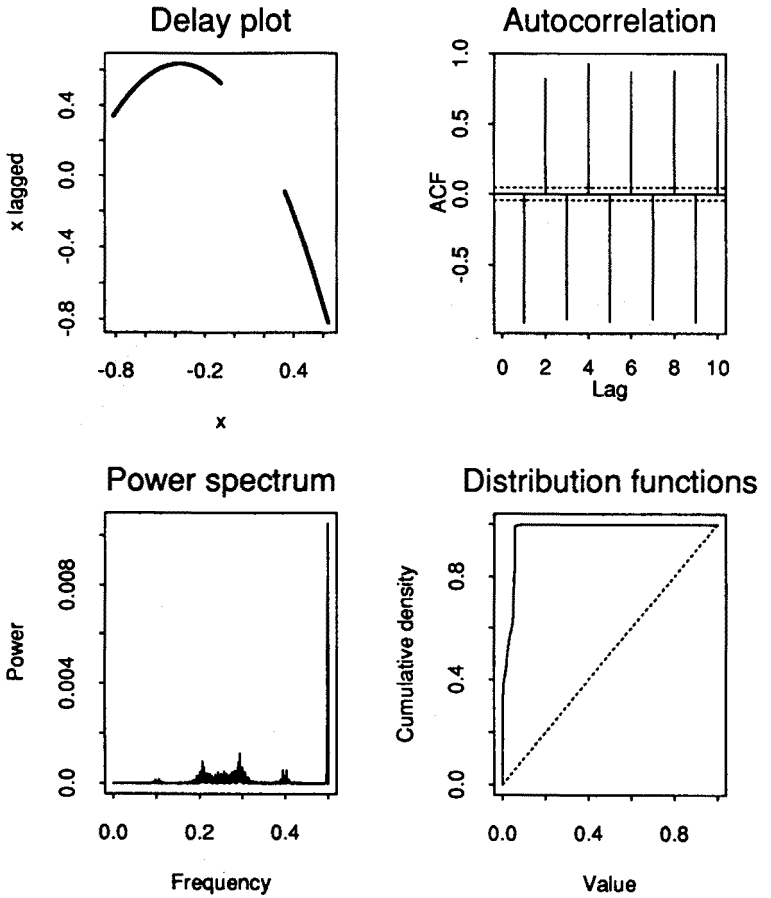

Fig. 12. Statistical analysis of the time series, $a = 1.45$ and $p = 1$. For the description, see text. Note the change in the horizontal scale on the autocorrelation plot. The 0.5 frequency peak (corresponding to the period 2) was removed in order to show the rest of the spectrum.

Fig. 11 and Fig. 12 present the results of the statistical analysis of the time series generated by Eq. (7), for $\mathcal{T} = 1 - ax^2$ with $a = 1.45$ (two-band

chaos). The results show clearly that for this a and p, the series is far from white noise limit, and that there are significant time correlations.

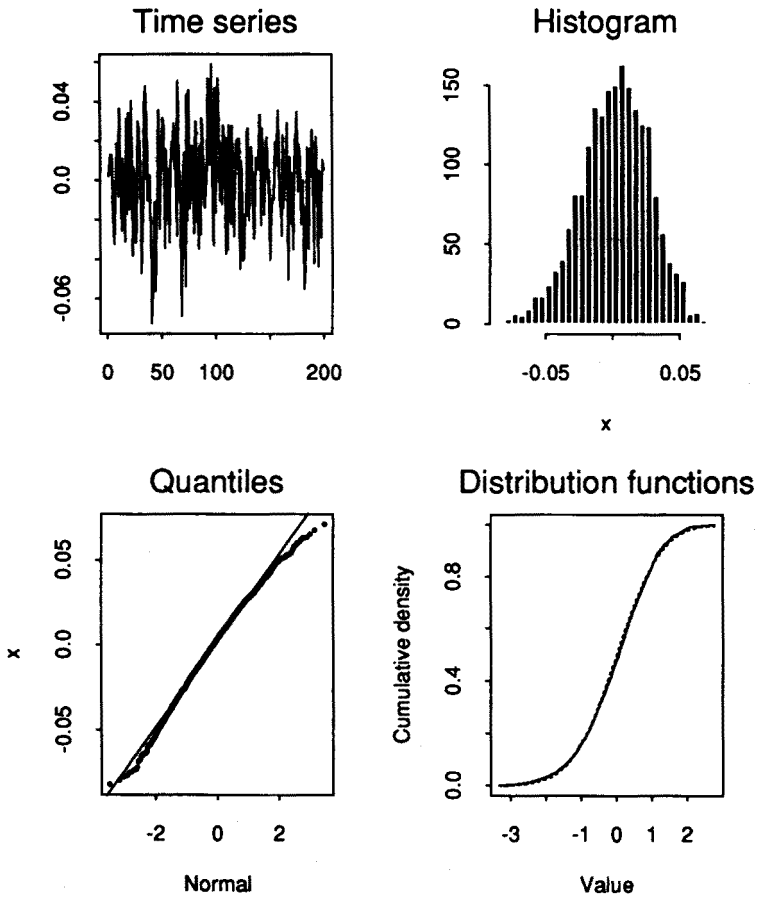

Fig. 13. Statistical analysis of the probability distribution, $a = 1.45$ and $p = 100$. For the description, see text.

On the other hand, for $p = 100$, the distribution is Gaussian, and the

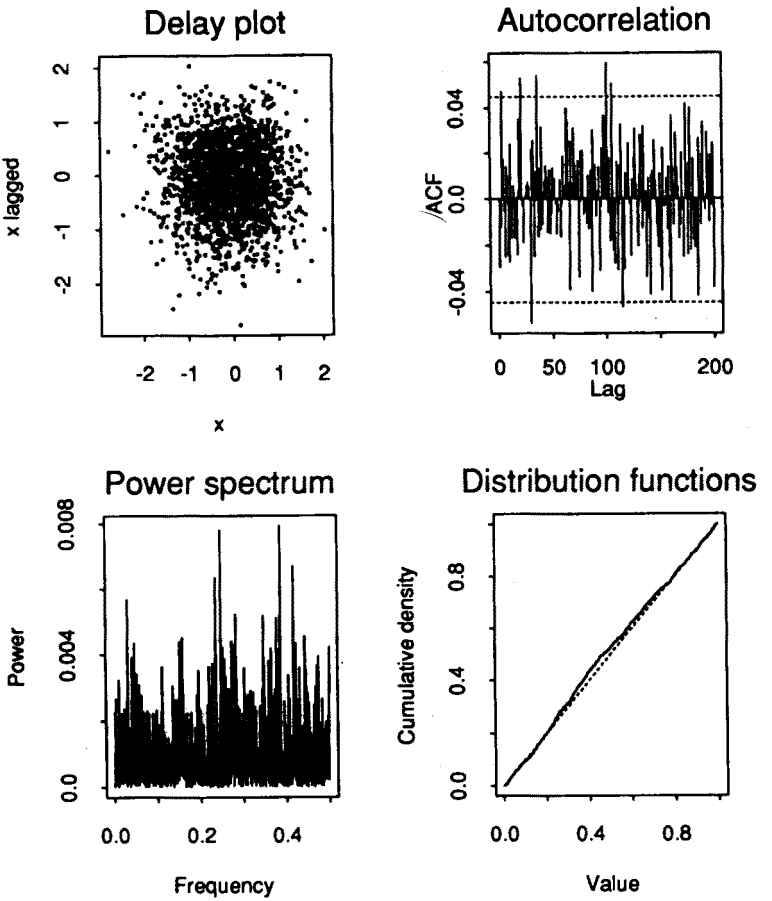

Fig. 14. Statistical analysis of the time series, $a = 1.45$ and $p = 100$. For the description, see text.

spectrum becomes flat, as shown in Fig. 13 and Fig. 14. There are still some short time correlations, but they are not very significant (the most prominent is the reminder of the negative correlation at 1 step forward from Fig. 12). The spectrum differs from the white noise spectrum, but

again, the differences are much less significant than on the previous plot.

As in the preceeding chapter, we can also analyze the Kolmogorov–Smirnov probabilities as a function of both a and p. Apart from the values of a which produce periodic (non-chaotic) solutions of the logistic map, all other values generate a good approximation of the Gaussian white noise for $p = 100$. On the other hand, for $p = 1$ the only one statistics significantly different from 0 is for the white-noise test for $a = 2.0$.

5. Chaotic characteristics

There is a number of different characteristics of chaos which can be analyzed here. The simplicity of the system allows us to find some of them in an analytical way, and to discuss the transition from chaotic, low-dimensional regime into the noise. This may be useful in understanding the properties of noise.

Let us first estimate the Lyapunov exponents spectrum, for the Eq. (1) with the perturbation given by Eq. (7). The full transformation can be written in the "memoryless" form by substitution $z_n^i = x_{n-i}$ for $i = 1 \ldots p$, and $z_n^0 = x_n^+$.

Then $z_n^i = \mathcal{T}^p z_{n-1}^i$, where $\mathcal{T}^p$ stands for the p-th iteration of $\mathcal{T}$, and the rest of the map can be written in the form

$$z_{n+1}^0 = \frac{\alpha + \beta z_n^0}{(\alpha + \beta z_n^0)(1 - \exp(-\gamma \sum_{i=1}^p z_n^i)) + \exp(-\gamma \sum_{i=1}^p z_n^i)}, \qquad (14)$$

with $\alpha = 0.5\,(1 - \mathrm{e}^{-T})$, $\beta = \mathrm{e}^{-T}$, and $\gamma = \epsilon T^{1/2} p^{-1/2}$. The Jacobi matrix has an upper triangular form, with

$$\frac{\partial z_{n+1}^0}{\partial z_n^0}$$

as the first element on the diagonal, and $\mathcal{D}$ as all other elements. $\mathcal{D}$ is an operator of a derivative of $\mathcal{T}$. For $\mathcal{T}v = 1 - a\,v^2$ it is equal to

$$\mathcal{D}v_n = (-2)^p v_{n-1} v_{n-2} \ldots v_{n-p},$$

with $v_n = \mathcal{T}v_{n-1}$.

The form of the matrix makes it possible to reduce the problem of finding the Lyapunov exponents to the calculation of the exponent for the equation (14), the remaining p exponents being equal to $p\lambda$ each, with λ being the exponent for $\mathcal{T}$.

Fig. 15 shows the values of the first component of the Lyapunov spectrum, *i.e.* the negative exponent generated by the genetic map, as a function

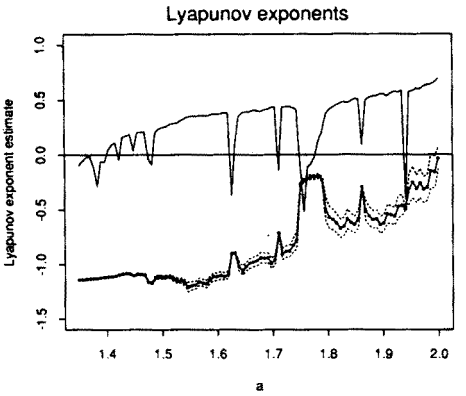

Fig. 15. Estimations of Lyapunov exponents for the genetic component of the model (lower curve), and for the logistic map (upper curve). Dotted lines show the variations in estimations for the genetic map (Lyapunov exponent being a mean of the time series of derivatives, and the lines here showing a variance).

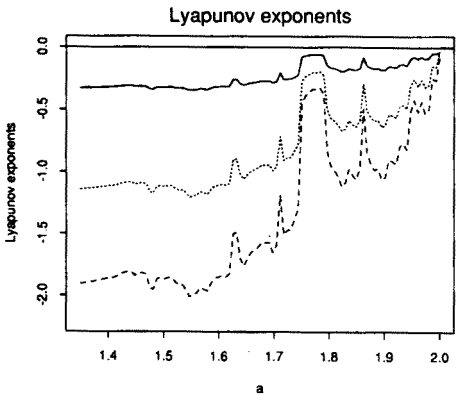

Fig. 16. The same as above, but for different p and ϵ: ___ — $p = 10$, $\epsilon = 3$; ... — $p = 100$, $\epsilon = 3$; - - - - — $p = 100$, $\epsilon = 5$.

of a, and compares it with the logistic map. In this simulations $T = 0.01$, $p = 100$, and $\epsilon = 3$. The length of simulations was 50000 for the genetic map (*i.e.* 500 in "natural" time units, and up to 5×10^6 for chaotic part).

With p changing, the first Lyapunov exponent for the genetic map also changes, but the general shape remains constant, *cf.* Fig. 16. Changing ϵ (and T) also changes the scale rather than a shape.

Finally, we used the existing numerical method of estimating the largest Lyapunov exponent from the time series (or, rather, expansion rates) [29], in order to check whether the data generated by the genetic model are indistinguishable from noise. Fig. 17 shows the results for the analysis for the embedding dimension 6 and the length of the time series of 2000. It is

clear that for large p the signal approaches the white noise (generated here by a standard *Splus* [30] procedure), although the structural differences generated by the genetic component can still be seen (as the levelling off of the plot).

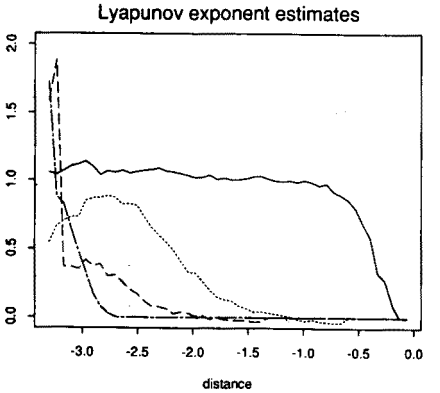

Fig. 17. Wilson and Rand estimates of the Lyapunov exponent (horizontal axis represents the distance by which the initial trajectory is perturbed, on the $\log_{10}$ scale, vertical axis represents the average expansion rate at this distance): ___ — Logistic, ... — $p = 1$, — — — — $p = 100$, — · — · — — noise.

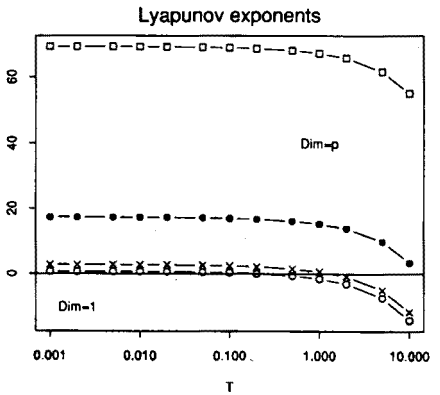

Fig. 18. Sum of all Lyapunov exponents of the system as a function of T for different p: $\circ - p = 1$, $\times - p = 2$, $\bullet - p = 5$, $\square - p = 10$; $\epsilon = 3.0$, $a = 2.0$. The Kaplan–Yorke dimension is p above the zero line, and 1 below.

The discussion of the dimensions was already given in [1]. For large p (corresponding to λ close to 1 in [1]) and small T, the time series is indistiguishable from the noisy one. However, for intermediate, and especially for small p and/or large T, there is a transition in dimensionality from simple,

one dimensional attractors pictured in Fig. 10, to apparently multidimensional objects from Fig. 9. The transition can be easily understood in terms of the Kaplan–Yorke dimension [20], which in our case is either 1, if the sum of all Lyapunov exponents is negative (here we have only one negative exponent for the genetic component of the map, and p equal exponents, negative or positive), and p otherwise. As shown in Fig. 15 and Fig. 16, the critical value is affected by all parameters of the map, *i.e.* p, T, and ϵ. Fig. 18 shows the sum of all Lyapunov exponents as a function of T for different values of p, for $a = 2.0$.

6. Final remarks

The approach to an analysis of dynamical systems with time–dependent perturbations as presented here is formed by two basic techniques, namely by the approximation of a time-depended signal by a series of impulses, and then by transforming the ordinary differential equation(s) into a discrete map by applying the stroboscopic maps formalism. The chaotic random number generator is also used in simulations of the stochastic process. The simple deterministic system generates the signal which is in the form suitable for the stroboscopic maps approach and which properties can be found analytically.

On the other hand, interesting results can be obtained even if we do not treat the procedures described above as the approximation procedures, and when we do no not take all the limits. This is especially true for the noise simulation, if the different stages of the approximation are treated literally. The series of attractors presented above and in [1] can be interpreted as the transition route from the case when the deterministic, chaotic dynamics being the actual source of the "noise" (as it is suggested in [3, 28]), can be seen by the "macroscopic" system, to the case when the separation of time scales "smears out" the chaotic motion, and the perturbation appears as a purely noisy process (in our case the Gaussian white noise, in [1] — the Ornstein–Uhlenbeck process). The conclusion (confirming the results of [3, 4, 28]) is that at least some of the stochastic processes (or manifestations of the processes, *e.g.* "noise-induced" transitions) in nature may be generated by deterministic systems, but the time scale separation makes them indistinguishable from the "purely" stochastic ones, if their action on other systems, correlation functions and distributions [3, 4], dimensions and entropies [28] are considered.

The author's stay in Cambridge was supported by the Royal Society (UK), the Wolfson Foundation, and the Foreign and Commonewealth Office. The program for calculating the largest Lyapunov exponent from a time

series was kindly provided by Howard Wilson. Ben Bolker provided the *Splus* code for performing Kolmogorov–Smirnov test, and helped the author in mastering the *Splus*.

REFERENCES

[1] E. Gudowska-Nowak, A. Kleczkowski, G.O. Williams, *J. Stat. Phys.* **54**, 539 (1989).
[2] A. Fuliński, E. Gudowska-Nowak, *Acta Phys. Pol.* **B22**, 457 (1991).
[3] C. Beck, G. Roepstorff, *Physica* **A145**, 1 (1987).
[4] C. Beck, *Nonlinearity*, **4**, 1131 (1991) and references therein.
[5] W. Horsthemcke, R. Lefever, *Noise-Induced Transitions*, Springer Verlag, Berlin 1984 and references therein.
[6] A. Kleczkowski, *Acta Phys. Pol.* **B24**, 1 (1993).
[7] K. Życzkowski, J. Zakrzewski, *J. Phys. A* **21**, L371 (1988).
[8] K. Życzkowski, *Phys. Rev.* **A35**, 3546 (1987).
[9] A. Carnagie, *J. Phys. B* **17**, 3435 (1984).
[10] J.G. Leopold, D. Richards, *J. Phys. B* **18**, 3369 (1985).
[11] R. Blümel, R. Meir, *J. Phys. B* **18**, 2835 (1985).
[12] E. Nelson, *Dynamical Theories of Brownian Motion*, Princeton University Press, Princeton NJ 1967.
[13] N.G. van Kampen, *Stochastic Processes in Physics and Chemistry*, North Holland, Amsterdam, New York, Oxford 1981.
[14] C. Gardiner, *Handbook of Stochastic Methods*, Springer Verlag, Berlin, Heidelberg, New York, Tokyo 1983, and references therein.
[15] H. Haken, *Synergetics: An Introduction*, Springer Series in Synergetics, Springer Verlag, Berlin, Heidelberg, New York, Tokyo 1984.
[16] C. van den Broeck, *J. Stat. Phys.* **31**, 467 (1983).
[17] R. Zygadło, *Acta Phys. Pol.* **A78**, 277 (1989).
[18] R. Zygadło, *Phys. Rev.* **E47**, 106 (1993).
[19] R. Zygadło, *Phys. Rev.* **E47**, 1993, in press.
[20] H.G. Schuster, *Deterministic Chaos. An Introduction*, Physik Verlag, Weinheim 1984, and references therein.
[21] N.S. Goel, N. Rychter-Dyn, *Stochastic Models in Biology*, Academic Press, New York 1974.
[22] E. Gudowska-Nowak, P.P. Szczęsny, *Acta Phys. Pol.* **B23**, 3 (1992).
[23] M. Lewenstein, T. Tél, *Phys. Lett.* **109A**, 411 (1985).
[24] W.H. Press, B.P. Flannery, S.A. Teukolsky, W.T. Vetterling, *Numerical Receipes, The Art of Scientific Computing*, Cambridge Univ. Press, Cambridge 1986, pages 455-459, and references therein.
[25] J.H. Zar, *Biostatistical Analysis*, Prentice-Hall Int., Inc., 2nd edition, 1984.
[26] M.S. Bartlett, *An Introduction to Stochastic Processes*, Cambridge Univ. Press, Cambridge, 2nd edition, 1966.

[27] W.A. Fuller, *Introduction to Statistical Time Series*, John Wiley & Sons, New York 1976.
[28] C. Beck, A. Kleczkowski, unpublished.
[29] H.B. Wilson, D.A. Rand, Detecting chaos in a noisy time-series. Warwick preprints, 16, 1993, submitted to: *Proc. Roy. Society* **B**.
[30] **Splus 3.1** by Statistical Sciences Europe, Oxford, UK.